Fabrication of arrays of plasmonic ‘top-hat’ structures using electron beam lithography

Shaoli Zhu[a,b], Han-Hao Cheng[b], Idriss Blakey[b, c], Nicholas Stokes[d], Kostya Ostrikov[e,f], Michael Cortie[a]

[a]Institute for Nanoscale Technology, University of Technology Sydney, PO Box 123, Broadway NSW, Australia, 2007

[b]Australian Institute for Bioengineering and Nanotechnology, University of Queensland, QLD, Australia, 4072;

[c]Centre for Advanced Imaging, University of Queensland, QLD, Australia, 4072

[d]formerly at Institute for Nanocale Technology, Sydney

[e]Plasma Nanoscience Laboratories, CSIRO Manufacturing Flagship, PO Box 218, Lindfield, NSW 2070, Australia

[f]School of Chemistry, Physics, and Mechanical Engineering, Queensland University of Technology, Brisbane, QLD 4000, Australia

ABSTRACT

Lithography techniques play an important role in the fabrication of nanoscale functional devices. In electron beam lithography (EBL) the determination of the optimum dose of electron irradiation is a very important parameter. In this paper, we first identify suitable EBL fabrication parameters by writing patterns with different sizes, periods and electron radiation doses. After finding suitable fabrication parameters, we show how five-pointed gold (Au) nanostructures with electric field-enhancing ‘top hats’ can be fabricated using EBL. Reflectance data of these arrays was measured in order to assess their potential applications in biosensing arrays.

Keywords: nano-star, electron beam lithography, exposure dose, optical properties

1. Introduction

Nanostructures with well-controlled shapes and sizes may be fabricated using focused ion beam (FIB) [1], electron beam lithography (EBL) [2,3] or nanoimprint lithography (NIL) [4]. Gold is a particularly suitable material of construction for such structures [5] especially using EBL which is capable of fabricating patterns down to about 10 nm resolution under ideal conditions [6]. Nanostructures made this way have potential applications in nano-electronic and photonic devices [7]. Poly(methylmethacrylate) (PMMA) is a common positive tone resist for EBL because it has a high resolution, good repeatability, and stability. [8,9] Typically PMMA has sensitivity of < 100 μC/cm^2 varying with the resist heights, the acceleration voltages, and the development procedures used [10]. Resolution limits [11], surface chemical modification effect [12] and photoresist effect [13] for the EBL fabrication process have been previously explored for simple shapes such as gold nanorods or deep

trenches. Unfortunately EBL in thick resist layers still suffers from the inevitable problem of low resolution due to broadening of the energy deposition profile of the electron beam inside the resist by electron scattering in the resist and the substrate [13]. Therefore it is still challenging to fabricate complex nanostructures using EBL.

In the present work, we investigated the optimum techniques to produce arrays of gold nano-stars for potential use in biosensing. In addition, we were interested in whether a reliable technique could be found to place a 'top hat' disk on top of a central hole within the nanostar. Such 'top-hats' have recently been reported to enhance the localised electric field on circular shapes [14] and they should also be effective on star shapes. We used two layers of PMMA to improve the lift-off success rate. Patterns with different sizes, periods and doses were designed. The effect of the spin coating parameters on the photoresist thickness and the substrate's effect on the dose requirements were also established. Finally, an array of complex gold nanostars was fabricated using EBL and the optical properties assessed.

2. Experimental

2.2 Dose test patterns

Patterns with different shapes, periods and doses were designed using ELPHY Quantum design software (Dortmund, Germany). As shown in fig 2, stars, star-holes, and star-star holes with different sizes, different periods and different doses (60 to 360 $\mu C/cm^2$) were created. The writing field size was 100 μm×100 μm. The dose factor is indicated by the colour of the stars and was varied on a row-by-row basis. Although stars of 1 μm, 1.5 μm, 2 μm and 3 μm were made, in the present paper we discuss only 1 μm size stars.

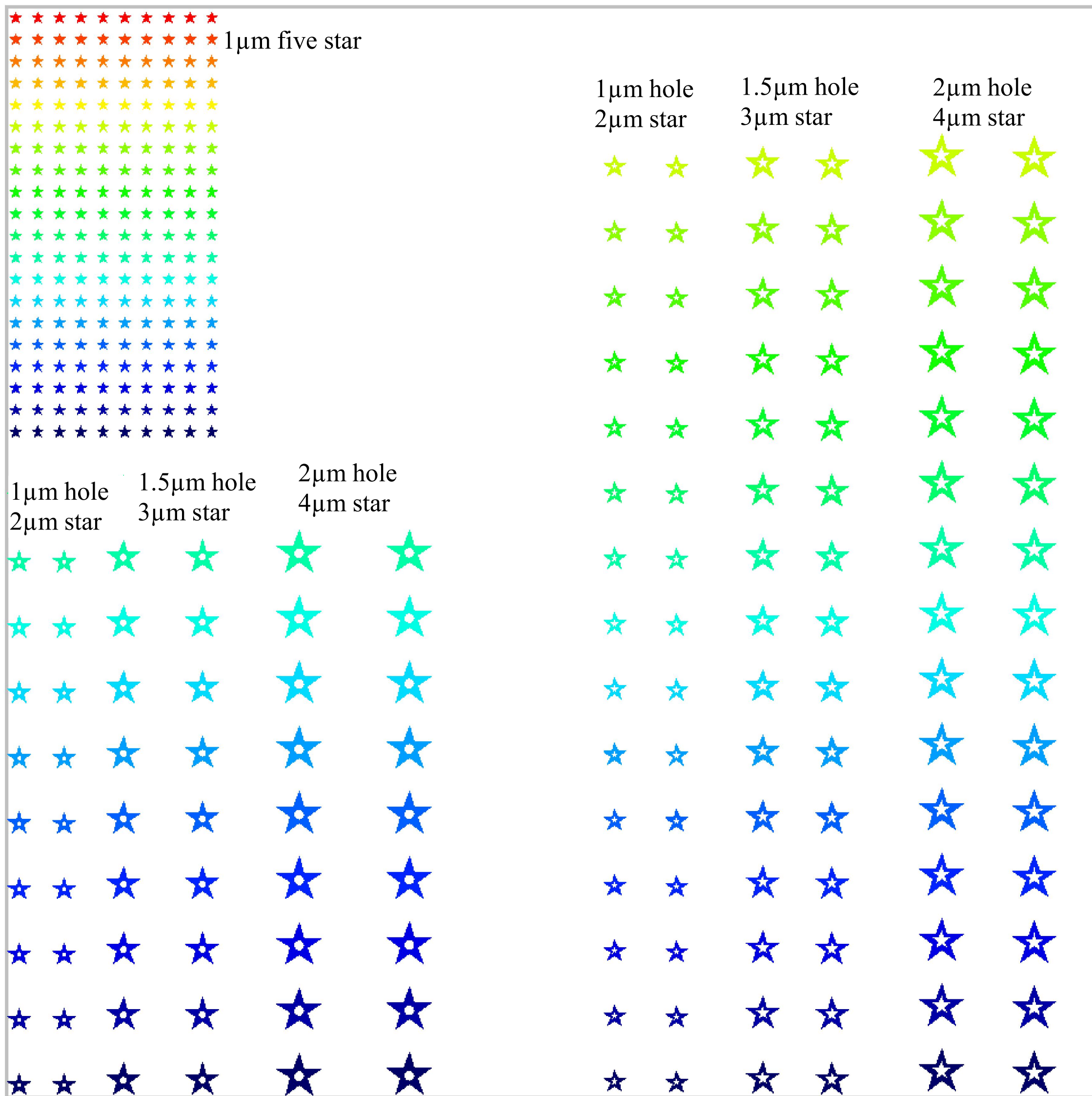

Fig 2. EBL pattern with different sizes, periods and doses, used to optimize dose.

2.3 Effect of substrate on dose requirements

Different substrates required different dose conditions and when a pattern was exposed on a new substrate, dose tests for that pattern were required. We initially investigated gold, silicon, glass and glass coated with ITO substrates to find which substrate was better for the fabrication of complex nanostructure arrays. Some insight was gained from use of the Casino modeling program V2.42 [15,16] to simulate the impact of 1000 electrons onto different substrates. In particular, collisions at the interface between the PMMA and the substrates were investigated. As shown in fig. 3, the number of backscattered electrons (BSE) increases significantly as the atomic number of substrate increased, with the BSE coefficient of a gold substrate being 0.47. BSE contributes to the PMMA chain scission and exposure. Therefore, the gold substrate requires a significantly lower dose than the other substrates. But the gold substrate has background noise, adhesion problems and a large grain size that contributes to increased surface roughness. The high yield of BSE generation can also result in a more severe ‘proximity effect’ during the patterning in the resist film. Although the ITO glass

substrate has more collisions and larger number of BSE paths than the silicon substrate, there are a larger number of collisions on the silicon substrate than the ITO glass substrate. Thus ITO dose required was slightly higher than that for silicon. From these results we can see that, of the three considered, silicon is the best substrate for EBL fabrication. Therefore, we selected silicon for the present work.

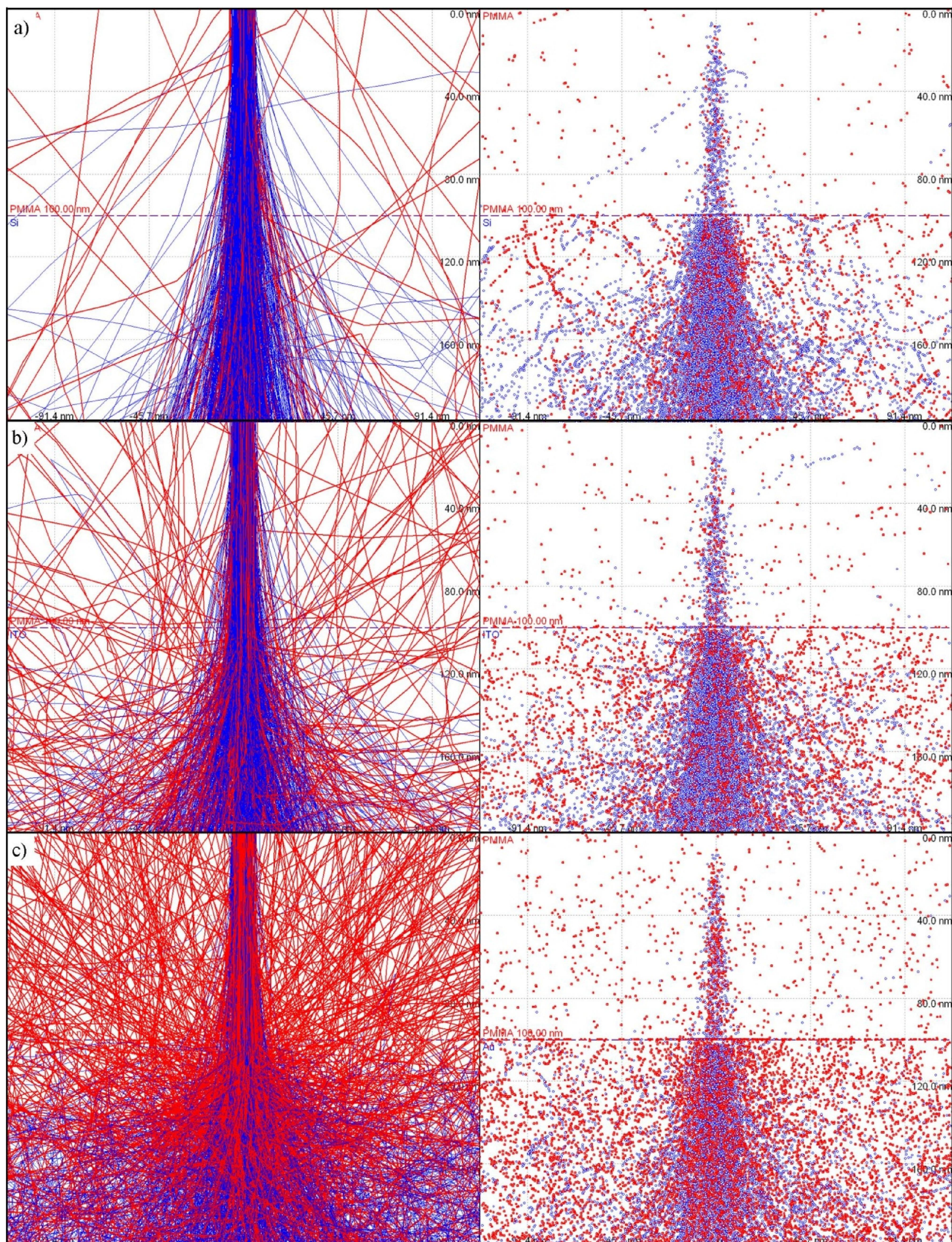

Fig 3. Thousand electron Casino simulations of 100 nm thick PMMA on substrates of (a) silicon, (b) ITO glass and (c) gold. The left column consists of the electron paths with blue the incident electrons and red the backscattered electrons and the right column show the collision points.

2.4. EBL fabrication

The EBL fabrication procedures are shown in fig. 4. First, p-type Si <100> wafers were cleaned by immersing in acetone and isopropanol alcohol for 2 min under sonication, followed by drying with a stream of N_2. The wafers were spincoated with bi-layer polymethylmethacrylate (PMMA) photoresists in which 4 wt% 495k and 2 wt% 950k PMMA (Microchem GmbH) were used for bottom and top layer resists. The solvent used in this case was anisole. Each layer of resist was soft-baked at 185 °C for 10 min on a hot plate after spin coating. Measurements with an ellipsometer indicated that the thickness of bi-layer PMMA was about 100 nm (±10nm). The wafers were exposed in a customised EBL system containing a Raith Elphy Quantum system attached to a JEOL-7800 FE-SEM. The exposures were carried out in the EBL system with acceleration voltage of 20 kV and with dose ranging from 60 to 360 $\mu C/cm^2$. The wafers were then developed in a solution containing a 1:3 ratio of methyl isobutyl ketone (MIBK) and IPA at room temperature for 31 seconds followed by rinsing in IPA and drying with N_2. The wafers were deposited with 5 nm of titanium (Ti, vacuum: 2×10^{-6} Torr, deposition rate 0.4A/sec) and 40 nm of gold (Au, vacuum: 2×10^{-6} Torr, Deposition rate: 1.5A/sec) using Temescal FC-2000 E-beam evaporator (Netherton Road Langbank Renfrewshire, Scotland-PA14 6YG, UK), followed by stripping the resist in acetone overnight. (The Ti layer is used to adhere the Au to the surface of the silicon wafer.)
The fabricated devices were then characterised under the JEOL 7800 SEM at 10-15 kV using the upper secondary electron detector (UED). We used ImageJ software (http://imagej.nih.gov/ij/) to measure the radius (*r*) of the tips of the stars. The reflectances of the various structures were measured with a SCI FilmTek 2000M (Temescal Headquarters, United States) using a 10X objective.

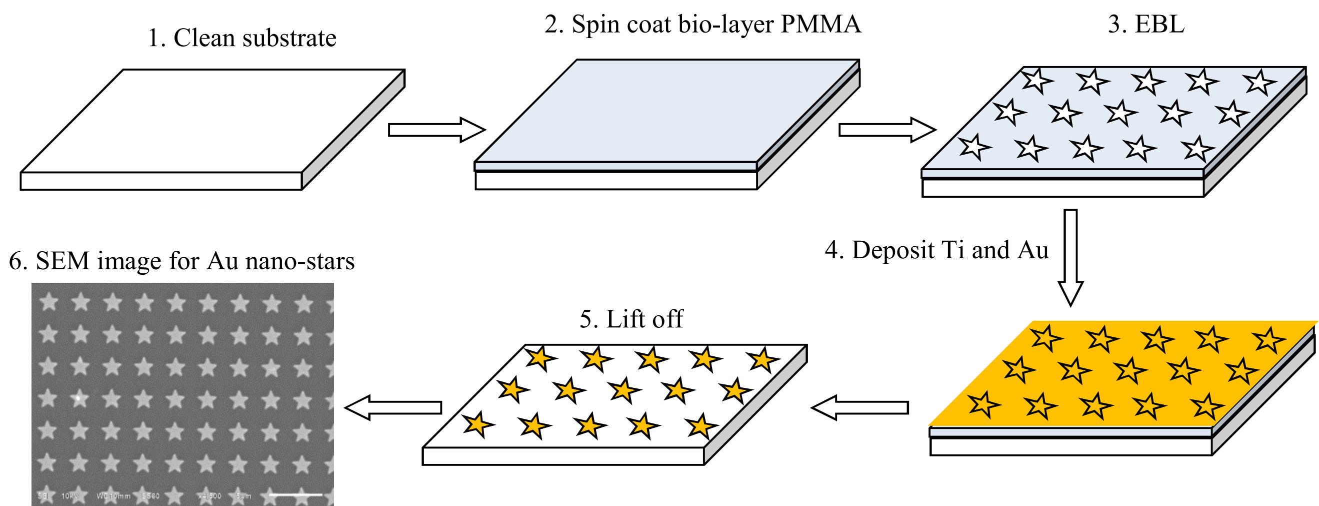

Figure 4. Illustration of electron beam lithography (EBL) fabrication procedures.

3. Results and discussion

3.1 EBL fabrication results

In the EBL fabrication process, dose factors of 60 to 360 μC/cm^2 were simultaneously evaluated in a single fabrication. The full SEM image of PMMA before lift off is shown in fig 5.

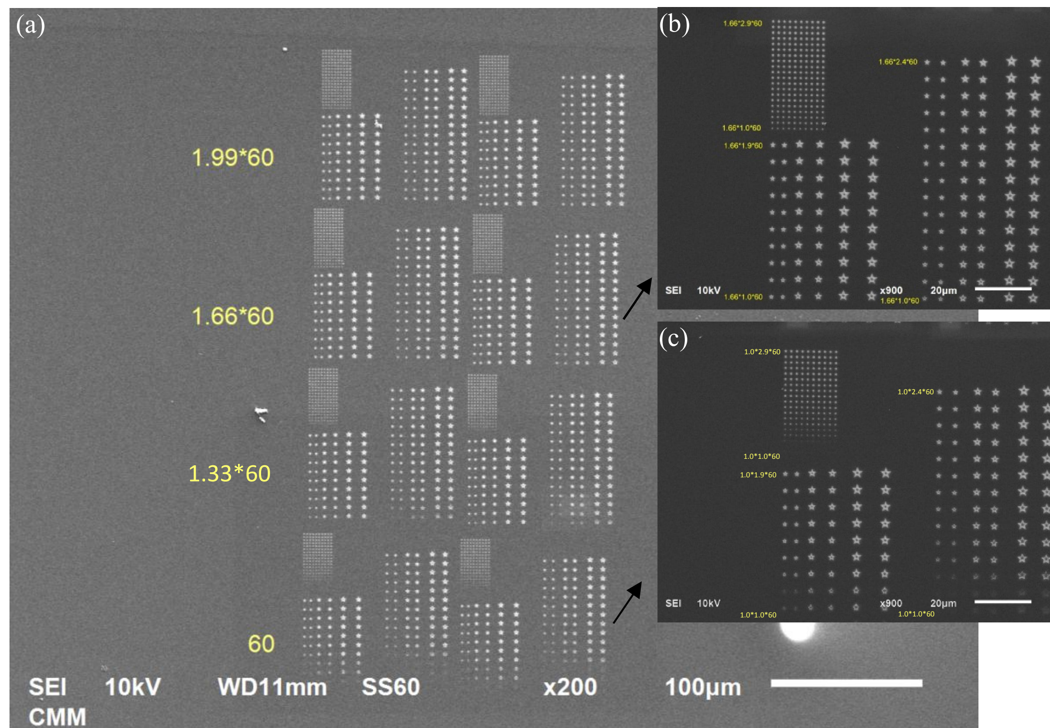

Fig 5. SEM image of PMMA pattern used for finding suitable EBL fabrication parameters for size, period and dose. (a) large area of patterns, (b) higher dose patterns, (c) lower dose patterns

Figure 5 shows the effect of varying fabrication parameters when attempting to write star structures onto PMMA. The desired dose was the lowest dose that produced complete structures. Figure 5(b) shows the region of patterns produced with higher doses. The patterns are sharp and distinct when the exposure doses are more than 200 μC/cm^2. Figure 5(c) indicates the patterns produced with lower dose, where some of the parts on the star structures are missing. We found that the optimum dose for the five-pointed star structures is about 220 to 230 μC/cm^2. Fig. 6 shows the SEM images after EBL fabrication with such a dose. Fig. 6 (a) is the SEM image for star shape. Fig. 6 (b) is star with circle hole pattern. Fig. 6 (c) is the SEM image of star with star hole. All examples mentioned are of the patterns on the PMMA resist before lift-off. SEM images of the samples after lift-off and deposition of 5 nm Ti and then a nominal 40 nm Au are shown in fig. 6 (d), fig. 6 (e) and fig. 6 (f). (AFM measurements showed that the thickness of the gold deposited varied somewhat over the surface of the silicon wafer, ranging from 40 to 80 nm.) From fig. 6, we can see that the PMMA patterns are more uniform than the subsequent Au nanostructure array. The whole size of star is about 1000 nm. The top-hat structures are about 500 nm. The radii of the tips of the Au nanostructures are less than 50 nm. After lift off, there are circle and star

nanostructures located on the top of the star pattern. This produces 'top hat' nanostructures (shown in fig.6 (e) and fig. 6 (f)). The reason that these structures form is that there is still some interconnection of the Au material which prevents the 'hat' from coming loose. The result is the interesting 3D structures seen here.

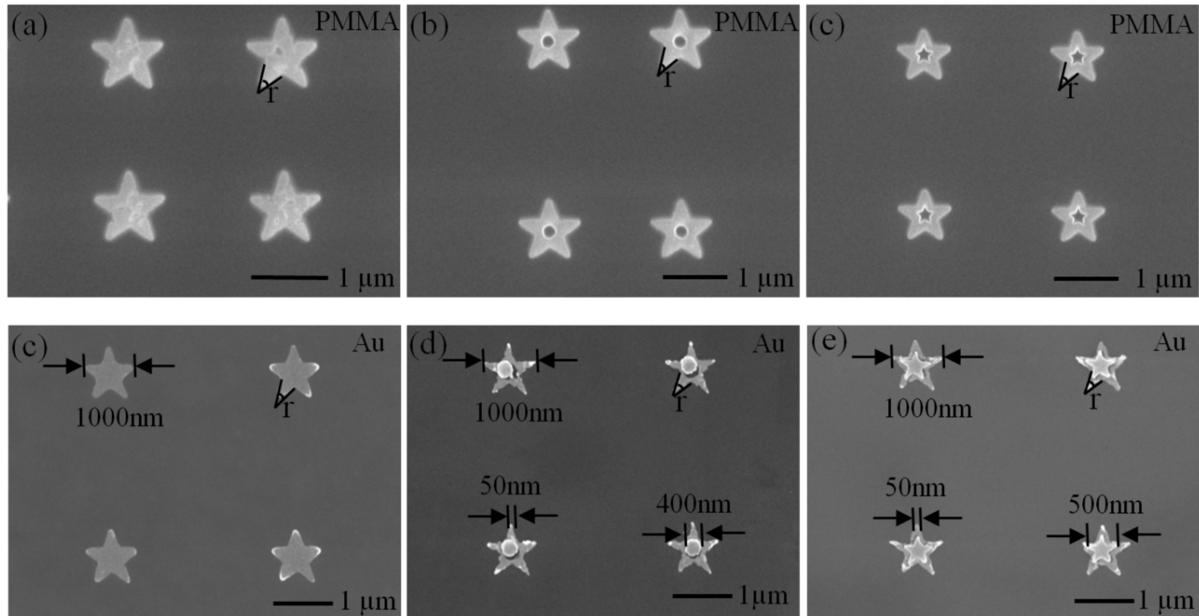

Fig 6. SEM images on PMMA before lift off (a) star, (b) star with circle hole, (c) star with star hole; and after lift off nanostructures (d) Au star, (e) Au star with circle top-hat, (f) Au star with star top-hat.

The presence of the hole has an effect on the radius of the tips of the star patterns in the PMMA but not once the gold has been deposited, fig. 7. The formation of the 'top hats' is schematically illustrated in Figure 8.

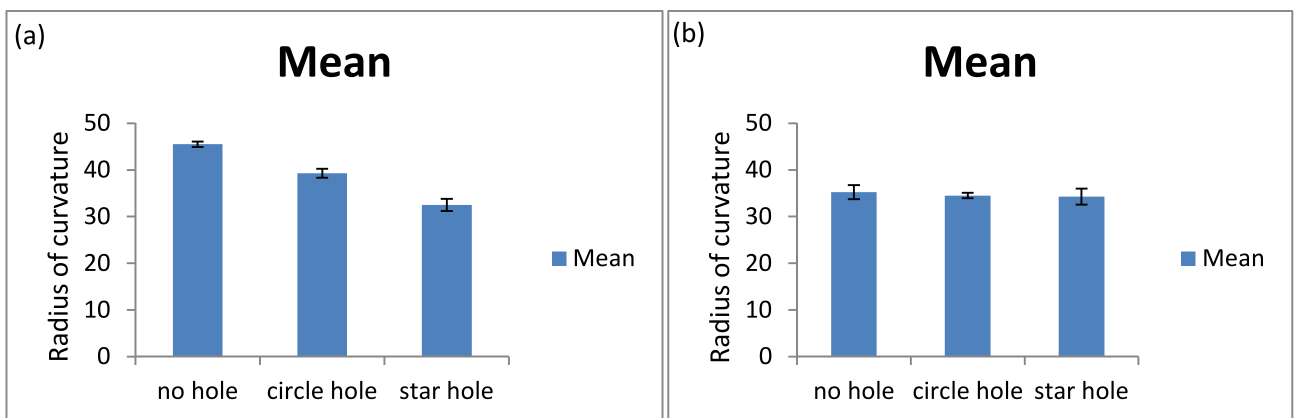

Fig 7 Radius of the curvature with error bars (a) before lift off (PMMA), (b) after lift off (Au star)

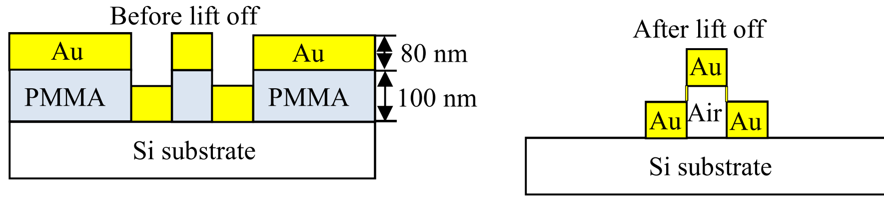

Figure 8. Schematic diagram illustrating formation of 'top hats'.

3.2. Optical properties

The reflectance of an array of Au stars with no top-hat (fig 9 (a)), circular top-hat (fig 9 (b)) and with star-shaped top-hat (fig 9 (c)) was measured by a reflectometer. Three fields were measured on each and the results averaged. In the absence of a top hat (fig. 9(a)), the reflectance increases towards the infrared and there is no clear evidence of a plasmon resonance within the visible range. Fig. 9 (b) shows the reflectance of the Au star with a circular top-hat. In this case there is a clear plasmonic resonance wavelength at around 550 nm and a significant absorption peak at about 550 nm. Fig. 9 (c) shows the reflectance of the Au star with star-shaped top-hat. There are two peaks (480 nm and 610 nm) in this graph which indicates that there are multiple resonances in the star top-hat structures. In addition, incorporation of a top-hat has caused the reflectance of light to decrease across all of the wavelengths investigated.

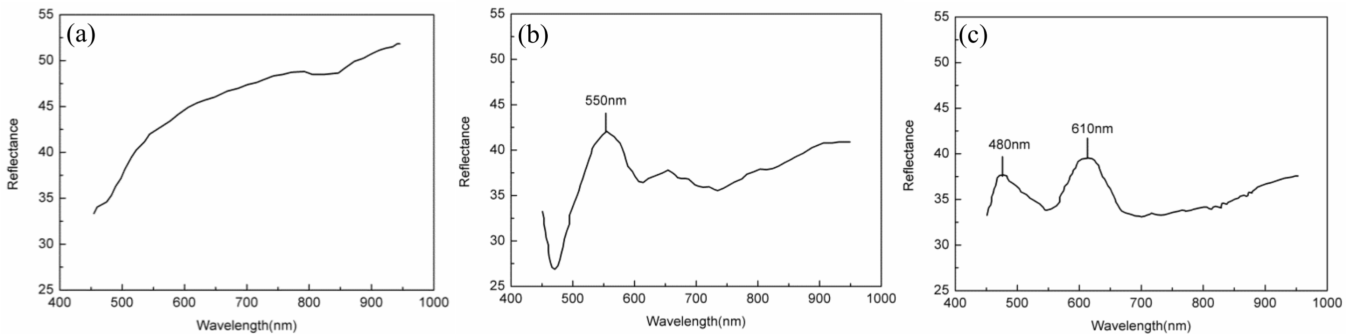

Fig 9. Reflectance for the Au star nanostructures (a) no top-hat, (b) with circle top-hat (c) with star top-hat

4. Conclusions

In this paper, we describe how complex five-pointed nanostructures with 'top-hats' can be produced in gold using electron beam lithography. The dose required was optimized using a test raster pattern which sampled a range of electron beam intensities. The choice of substrate was optimized using a Monte Carlo simulation. The resulting five-pointed gold stars have tips with radii of the about 50 nm, and a nominal height of about 40 nm. The reflectance spectra are significantly effected by the presence of a 'top-hat' and, if present, by its shape. The optical properties of this nanostructure show that it has potential applications in plasmonic nanobiosensors based on either refractometric or surface enhanced Raman transduction.

Acknowledgement

S.Z. acknowledges the support of postdoctoral fellowships provided by the University of Queensland (FT10942050) and by University of Technology Sydney (ARC DP120102545). The experimental work was performed at the University of Queensland node of the Australian National Fabrication Facility (ANFF-Q), a company established under the National Collaborative Research Infrastructure Strategy to provide nano and micro-fabrication facilities for Australia's researchers, and at the Centre for Microscopy and Microanalysis at the University of Queensland. K.O. acknowledges partial support from the Australian Research Council and CSIRO OCE Science Leadership Program. The Monte Carlo simulations were performed by N.S. (ARC Linkage project LP0560475).

REFERENCES

[1] K. Arshak, M. Mihov, A. Arshak, et al, *Microelectro. Eng.* 73 (2004) 144-151.
[2] W. Langheinrich, H. Beneking, *Microelectro. Eng.* 13 (1991) 225-228.
[3] M. Peckerar, R. Bass, K.W. Rhee, *J. Vac. Sci. Technol. B* 18 (2000) 3143-3149.
[4] H. Schift, *J. Vac. Sci. Technol. B* 26 (2008) 458-480.
[5] N. Stokes, A. M. McDonagh & M. B. Cortie, *Gold Bull.* 40 (2007) 310-320.
[6] H. Duan, H. Hu, H.K. Hui, Z. Shen, J.K.W. Yang, *Nanotechnology* 24 (2013)185301.
[7] D. Dregely, F. Neubrech, H. Duan, R. Vogelgesang, H. Giessen, *Nat. Commun.* 4, (2013) Article number:2237.
[8] S. Thoms, D. S. Macintyre and M. McCarthy, Microelectron. Eng. 41/42 (1998) 207–210.
[9] M. A. Mohammad, K. Koshelev, T. Fito, D. A. Zheng Z, M. Stepanova and S. Dew, *Jpn. J. Appl. Phys*.51 (2012) 06FC05.
[10] K. Koshelev, M. Ali Mohammad, T. Fito, K. L. Westra, S. K. Dew and M. Stepanova, *J. Vac. Sci. Technol.* B 29 (2011) 06F306-01
[11] V. R. Manfrinato, L. Zhang, D. Su, H..Duan, R. G. Hobbs, E. A. Stach,and K. K. Berggren, *Nano Lett* 13 (2013) 1555−1558.
[12] Z. Zhang , H. Duan , Y. Wu, W. Zhou, C. Liu, Y. Tang, H. Li, *Microelectro. Eng.* 128 (2014) 59–65.
[13] M. Sarkar, Y.N. Mohapatra, *Microelectro. Eng.* 130 (2014) 1–7.
[14] V. G. Kravets, G. Zoriniants , C. P. Burrows, F. Schedin, A. K. Geim, W. L. Barnes and A. N. Grigorenko, *Nano Lett.*, 2010, 10 (3), pp 874–879
[15] D. Drouin, A. R. Couture, D. Joly, X. Tastet, V. Aimez, R. Gauvin, CASINO V2.42: a fast and easy-to-use modeling tool for scanning electron microscopy and microanalysis users. Scanning. 2007 May-Jun;29(3):92-101
[16] Demers H, Poirier-Demers N, Couture AR, Joly D, Guilmain M, de Jonge N, Drouin D. Three-dimensional electron microscopy simulation with the CASINO Monte Carlo software. Scanning. 2011 May-Jun;33(3):135-46. doi: 10.1002/sca.20262. Epub 2011 Jul 18.